SENSOR-DRIVEN ANALYSIS OF ANGLE OF ATTACK IN ALPINE SKIING: A LABORATORY EXPLORATION

Sebastian Schütz[1], Patrick Thorwartl[2], Helmut Holzer[3], Thomas Stöggl[4], and Christoph Thorwartl[5]

Department of Geoinformatics, University of Salzburg, Austria[1]
Wöss Ladenbau – Metalltechnik GmbH, Austria[2]
Atomic Austria GmbH. Austria[3]
Red Bull Athlete Performance Center, Austria[4]
Salzburg Research Forschungsgesellschaft m.b.H., Austria[5]

The aim was to address the absence of a universal measuring instrument for detecting the degree of carving or skidding in a ski turn. Sensors were employed to calculate the so-called angle of attack (θ), which increases if lateral skidding increases. A mathematical concept in 2D and 3D for sensor-based detection of the θ was developed and evaluated on a self-built centrifugal machine capable of executing both optimal carving as well as certain degrees of skidding. The variation of θ was systematically divided into the stages small, medium, and large. Each stage was further subdivided into three smaller levels to evaluate the discriminability of minor changes. Across all settings with different θ values, both 2D and 3D methods demonstrated precise recording and discrimination of subtle differences (1°-1.5°), as confirmed by 95%-Confidence Intervals.

KEYWORDS: alpine skiing, angle of attack, GNSS, IMU, prototyping, ski trajectory.

INTRODUCTION: The way in which a ski interacts with the snow surface reveals valuable information about the quality and performance of a turn. When a ski moves laterally while moving forward on the snow, it is referred to the technique “skidding”. In contrast, a carving turn is characterized by the ski experiencing minimal to no sideways movement relative to its trajectory. As a result, a point along the ski edge follows the same path as the preceding one; this defines a modern carving turn (Brown & Outwater, 1989; Lieu & Mote, 1985; Reid, Haugen, Gilgien, Kipp, & Smith, 2020; Renshaw & Mote Jr, 1989). In technical terms, difference between the orientation vector of the ski ($\vec{E}$) and the resultant velocity vector ($\vec{v}$) induces skidding. The corresponding angle between $\vec{E}$ and $\vec{v}$, known as the angle of attack (θ), ideally equals zero in a perfect carving turn. However, achieving a physically flawless carving turn is challenging; instead, authors have identified temporal variations in θ and ski deflection across different segments of the ski (Reid et al., 2020; Thorwartl et al., 2023). Reid et al. (2020) recently delved into this matter in depth; however, the undertaking was quite laborious. Employing a videographic system equipped with four synchronized cameras and 228 control points, the study recorded 12 turns within a specified corridor. While the findings contribute significantly to the comprehension of the interplay between skis and snow, the measurement setup is impractical for routine training due to its material and time requirements. So far, a measurement instrument for the straightforward determination of θ is lacking. This study seeks to assess a new sensor-based method using Inertial Measurement Units (IMUs) and a Real-Time Kinematic (RTK) Global Navigation Satellite System (GNSS) to measure the θ within a controlled laboratory setting. Consequently, the objective of this work is to (i) identify a sensor-based solution for θ detection in 2D and 3D, and (ii) to proof the precision of this approach using a self-developed centrifugal machine.

METHODS: A ski (Atomic Redster G7; length: 1.75 m; radius: 16.2 m) was equipped with two IMUs from Xsens (DOT sensor) and a GNSS (Xsens, MTi-680G). The GNSS sensor's antenna was fastened to the rear section of the ski, precisely positioned 68 mm from the tail. To simulate a carving (θ very close to 0°) and different stages of skidding (θ > 0°), a ski centrifugal machine was constructed and manufactured. Instrumentation of the ski on the centrifugal machine is

facilitated by two chains, allowing variation of the θ by adjusting the length of the front chain (refer to Figure 1). The ski is rotated by an alternating current motor (TRAMEC Getriebe GmbH, SFK 40) with a worm gear unit. The ski's rotation speed, set to approximately 7.5 m/s, was achieved using a frequency converter (FC) (Yaskawa Europe GmbH, GA 500). The variation in the ski's θ was systematically split into small, medium, and large settings. Each of these three stages was further discriminated into three smaller levels, yielding the following estimated θ settings: small (S1 = 0°, S2 = 1.5°, S3 = 2.9°), medium (M1 = 11.6°, M2 = 13.1°, M3 = 14.5°), and large (L1 = 23.2°, L2 = 24.7°, L3 = 26.1°). It's important to note that these values were determined geometrically based on the shortening of the chain with straight skis, unlike the bent configuration used in the test setup. Each θ setting was executed for a duration of 45 s, and only the central 25% of the data was utilized for analysis, taking into account the system's acceleration and deceleration requirements. For a visual verification of the detected θ, a camera (GoPro Hero) was positioned to capture footage of the ski from an overhead perspective (Figure 1).

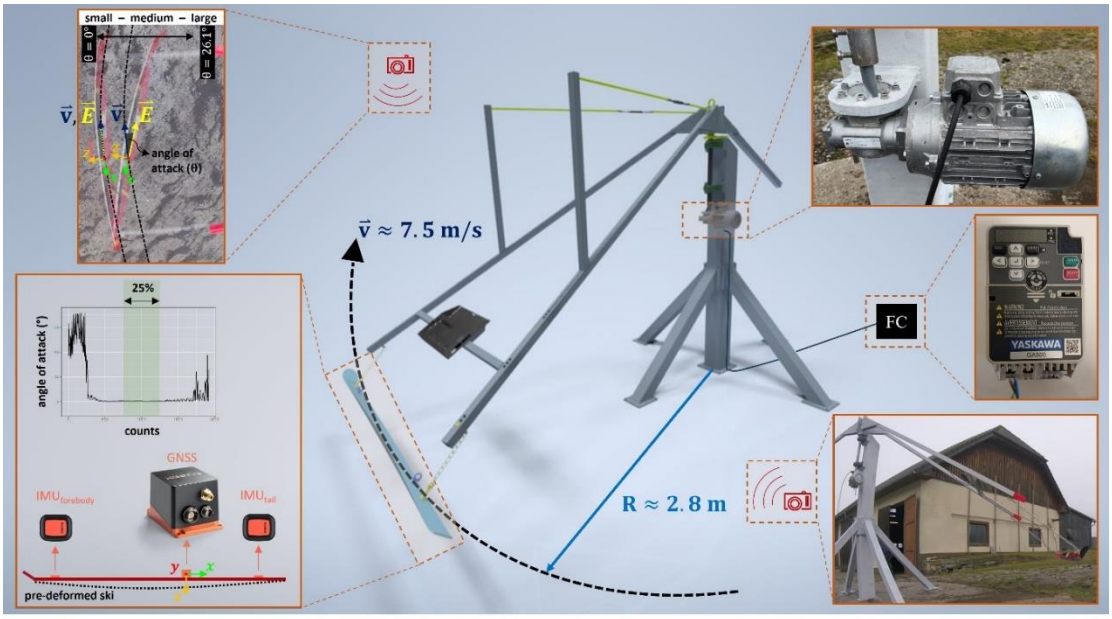

Figure 1: Measurement setup

All data was measured at 20 Hz. The IMU data was recorded time-synchronously using the Xsens DOT app and stored on a mobile device. For overall synchronization with GNSS a reference movement, represented by a quick vertical up and down movement of the whole ski, was performed at the beginning of each measurement. Using the cosine-similarity measure of the acceleration data during this unique movement allowed satisfying overall synchronization of the data. Position signal of GNSS was corrected via Networked Transport of Radio Technical Commission for Maritime Services via Internet Protocol (NTRIP). Due to discrepancies in yaw (orientation in xy-plane) of IMUs and GNSS an initial correction was performed, i.e. the yaw of the IMUs were set to the value of the GNSS at the beginning of the measurement. No further filtering was applied. Orientation output of all sensors is provided drift-free due to internal filtering algorithms (e.g. Kalman). Orientation of the ski was computed using the angular position of the respective sensor (IMU forebody, IMU back and GNSS) (Figure 1). The $\vec{v}$ data was acquired through GNSS, with measurements taken in the East, North, and Up coordinate system, along with the measurement of $\vec{E}$. For comparison of settings 95% confidence intervals are presented along with boxplots. First, θ was calculated at a projection in 2D using the yaw angle (orientation in xy-plane) only, neglecting the pitch angle (orientation with respect to the z-axis). For 3D analysis, yaw of GNSS and pitch angle at the respective sensor position was

used to calculated angular differences. All calculations were done using statistical software R (version 4.3.2).

RESULTS: Figure 2a reveals a clear distinction between the main stages small, medium, and large. It is important to note that there was a sensor failure at setting S1, resulting in the unavailability of data. Although seen in boxplots, 95% confidence intervals show no pairwise overlaps among smaller levels indicating the statistical potential for discrimination. Similarly in 3D, Figure 2b shows visible changes for the main stages. It can also be observed that differences compared to 2D are greater at the large setting (L1-L3). Again, at each sensor position, levels can be statistically differentiated using 95% confidence intervals.

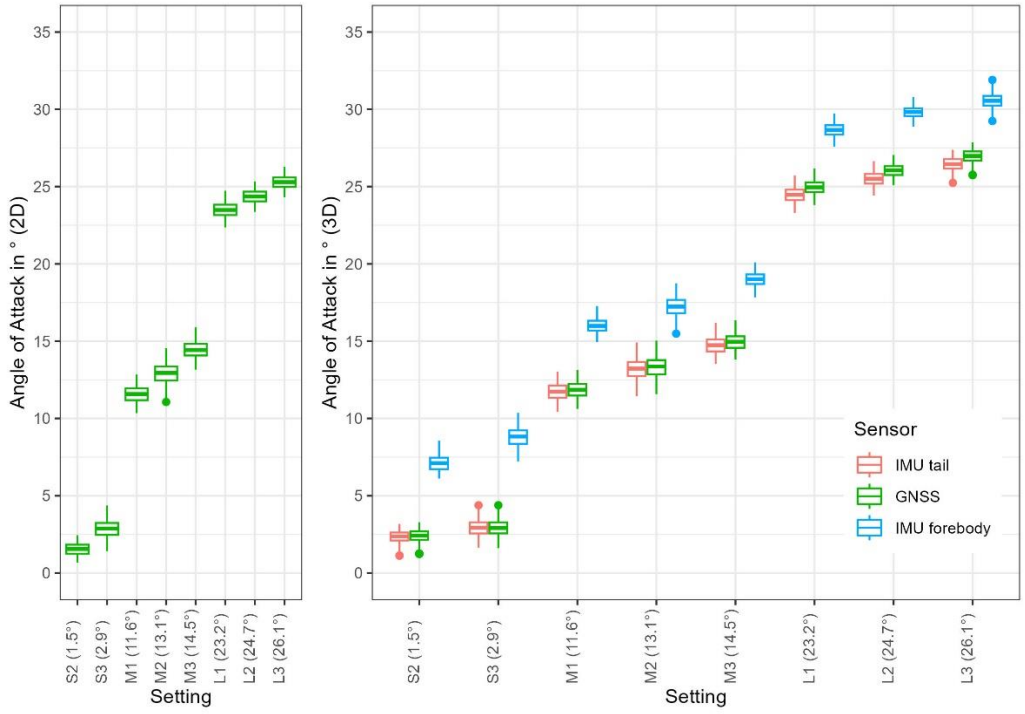

(a) **(b)**

Figure 2: Calculated angle of attack (θ) for (a) GNSS in 2D (without pitch angle) and (b) GNSS, IMU tail, and IMU forebody in 3D) for small (S), medium (M) and large (L) setting.

Overall, the values of θ for the IMU forebody are the highest for each setting, followed by GNSS and IMU tail (Table 1).

Table 1: 95% Mean and Confidence Interval (CI) of angle of attack (θ) for small (S), medium (M) and large (L) setting.

Setting		Mean (95% CI) of θ in 2D in °	Mean (95% CI) of θ in 3D in °		
		GNSS	IMU forebody	GNSS	IMU tail
S	1				
	2	1.5 (1.5 – 1.6)	7.0 (6.9 – 7.1)	2.5 (2.4 – 2.5)	2.5 (2.4 – 2.5)
	3	2.9 (2.8 – 3.0)	8.9 (8.8 – 9.0)	2.9 (2.8 – 3.0)	2.9 (2.8 – 3.0)
M	1	11.6 (11.5 – 11.7)	15.7 (15.7 – 15.8)	11.8 (11.7 – 11.9)	11.7 (11.6 – 11.8)
	2	12.9 (12.8 – 13.0)	17.2 (17.2 – 17.3)	13.3 (13.2 – 13.4)	13.2 (13.1 – 13.3)
	3	14.5 (14.4 – 14.6)	19.1 (19.0 – 19.2)	15.0 (14.9 – 15.1)	14.8 (14.7 – 14.9)
L	1	23.5 (23.5 – 23.6)	28.6 (28.6 – 28.7)	25.0 (24.9 – 25.0)	24.5 (24.4 – 24.6)
	2	24.4 (24.3 – 24.4)	29.8 (29.7 – 29.8)	26.0 (26.0 – 26.1)	25.5 (25.4 – 25.6)
	3	25.2 (25.2 – 25.3)	30.5 (30.5 – 30.6)	26.9 (26.9 – 27.0)	26.4 (26.3 – 26.5)

DISCUSSION: This study introduces a prototype based on GNSS and IMUs designed to detect the amount of skidding by determining not only the θ near the binding but also the local θ at the forebody and tail of the ski. Two methods were employed to calculate the θ: the 2D method, without pitch angle, and a 3D method. Currently, no universally applicable device exists to measure a ski's carving or skidding engagement, prompting a proof-of-concept study.
The results demonstrate that the θ can be measured at a satisfying level of correctness in a standardized environment, facilitating the discrimination of subtle variations across the measured configurations using both the 2D and 3D methodologies. Notably, there was no overlap of the 95% confidence interval across all settings, indicating a high degree of precision. Even small variations (1° - 1.5°) can be distinguished within the small, medium, and large settings. As a limitation, it should be noted that no comparison was made with a gold standard, which means that no definitive conclusions can be drawn regarding validity. However, when comparing the geometrically calculated θ (for the non-curved ski) with the θ measured at the position of the GNSS, a maximum deviation of 0.9° for 2D and 1.3° for 3D was found. Further validation measurements are planned to be conducted extensively.
Moreover, it was consistently observed across all settings that the local θ is larger at the front of the ski, followed by the GNSS, and the θ at the back of the ski. This finding aligns with earlier research indicating a slight elevation in the θ within the ski's forebody during an advanced carving stage (Federolf, Roos, Lüthi, & Dual, 2010; Thorwartl et al., 2023). However, it is conceivable that the local θ can be reduced for a specific human-equipment setting by optimizing fundamental design parameters, such as side-cut radius, and the progression of bending and torsional stiffness.
Whether plausible data can be detected in the field needs to be determined through additional in-field measurements. Furthermore, it is prospectively necessary to replace the current GNSS with a smaller device to avoid potential disruptions during skiing. Alternatively, it is conceivable to explore a machine learning approach to train the IMU in a way that it can calculate the θ even without GNSS. However, the $\vec{v}$, provided by the GNSS, is still required at present.

CONCLUSION: Analysing the local θ could open the door to a physics-based approach to product customization, since the θ proofs the definition of carving. The smaller the θ, the greater the proportion of carving, resulting in reduced energy dissipation and consequently enhancing the quality of a turn. The θ could be particularly interesting in the realm of ski material optimization and product fitting. It depends less on the dynamics of skiing, making it besides the high-end elite skiers also suitable for moderately skilled skiers who are not seeking performance improvement but rather aiming to find a suitable ski for safe skiing.

REFERENCES

Brown, C., & Outwater, J. O. (1989). On the skiability of snow. In R. Johnson, C. Mote, & M. Binet (Eds.), *Skiing trauma and safety: seventh international symposium, ASTM STP 1022* (Vol. 1, pp. 329-336). Philadelphia, USA: ASTM International.
Federolf, P., Roos, M., Lüthi, A., & Dual, J. (2010). Finite element simulation of the ski–snow interaction of an alpine ski in a carved turn. *Sports Engineering, 12*(3), 123-133.
Lieu, D., & Mote, C. (1985). Mechanics of the turning snow ski. In R. J. Johnson & C. D. Mote (Eds.), *Skiing Trauma and Safety: Fifth International Symposium* (Vol. 1, pp. 117–140). Philadelphia, USA: ASTM Internationale.
Reid, R. C., Haugen, P., Gilgien, M., Kipp, R. W., & Smith, G. A. (2020). Alpine Ski Motion Characteristics in Slalom. *Frontiers in Sports and Active Living, 2*, 25.
Renshaw, A. A., & Mote Jr, C. (1989). A model for the turning snow ski. *International journal of mechanical sciences, 31*(10), 721-736.
Thorwartl, C., Tschepp, A., Lasshofer, M., Holzer, H., Zirkl, M., Hammer, M., . . . Stöggl, T. (2023). Technique-Dependent Relationship between Local Ski Bending Curvature, Roll Angle and Radial Force in Alpine Skiing. *Sensors, 23*(8), 3997.

ACKNOWLEDGEMENTS: The authors would like to express their gratitude to Wöss and Atomic for their excellent cooperation. A special thank you is also extended to “Bananalgut” for providing the infrastructure support.